

## Encyclopaedia of the Anthropocene: Magnetic particulates as markers of fossil fuel burning

**Mark W. Hounslow**

Lancaster Environment Centre, Farrer Avenue, Lancaster University, Lancaster, UK., LA1 4YQ.

[M.Hounslow@lancaster.ac.uk](mailto:M.Hounslow@lancaster.ac.uk).

[Tel:+44 1524 701026](tel:+441524701026).

**Keywords:** coal, diesel, particulate pollution, fly-ash, hematite, lake sediments, magnetite, magnetic susceptibility, industrial revolution, peat, remanence, spherules, vehicle particulates.

### Abstract

Particulate matter derived from various sources of fuel combustion contains minor to trace amounts of Fe-oxides that can be detected by magnetic measurements. These magnetic particulates can be used as proxies for particulate pollution, since oxide contents are often larger in amounts and may have distinctive magnetic properties, compared to most types of natural dusts. Magnetic particulates range in size from a few nanometres to 100s of microns. Magnetic measurements of sediment cores and soils therefore provide evidence for historical particulate pollution loads, both in time since ca. AD 1800, and the spatial expression of pollution loads. {97 words}

### Main text

#### Inorganic particulate matter from fossil fuel burning

Particles in the atmosphere are derived from several sources, which include sea salt, biogenic aerosol particles, inorganic dusts (from soils, rocks, volcanic ash and anthropogenic activities) and combustion-derived particles (Gieré and Querol, 2010). Our use and burning of fossil fuels generates both carbonaceous particles and various kinds of inorganic dusts, emitted into the atmosphere, with a wide range of particle sizes from a few nanometres (nm) to several hundred microns ( $\mu\text{m}$ ) (Fig. 1). This large range of particle size is a reflection of the diverse modes of formation of these aerosols. Inorganic Particulate Matter (PM), can comprise both crystalline and amorphous particulate matter. Here a specific focus is on the crystalline PM, and its characterisation using magnetic methods (Petrovsky & Ellwood, 1999; Snowball et al., 2014). These magnetic properties are largely carried by magnetite ( $\text{Fe}_3\text{O}_4$ ) and like aerosol formation processes, magnetic behaviour is in part particle size dependent (Fig. 1).

Prior to the major utilisation of coal during the early parts of the industrial revolution, wood and charcoal burning would have been the major source of anthropogenic generated PM. This was added to during the 17<sup>th</sup> and 18<sup>th</sup> century, when coal (and oil shale) combustion, and the fly ash emitted by its burning, took over as the major source of inorganic PM dispersed in the environment from fuel combustion. As happening now and into the future, sources of anthropogenically-derived PM will change, as dominant fuel use changes away from coal. Magnetic methods of PM characterisation are receiving wider use, because of the non-destructive, simple and rapid

methodology (Petrovsky & Ellwood, 1999; Snowball et al., 2014). Magnetic particles (large Fe-rich) giving rise to these magnetic properties are inevitably embedded and intermixed with a wide variety of more dominant particle types from all kinds of pollution sources, so this topic will also examine magnetic particulates, as part of the larger range of inorganic PM properties.

### **Physical characteristics**

The relative abundance of carbonaceous PM and inorganic PM, emitted by primary fuel combustion, is dependent on the mineral content of the fuel, so mineral-poor fuels such as wood, oil and diesels tend to be rich in carbonaceous PM, whereas mineral-rich fuel such as coals and oil-shales tend to be rich in inorganic PM (Smith et al., 2012; Sanderson et al., 2014). This distinction is also expressed in the particle sizes with fly-ash generated by coal combustion rich in coarse PM  $>1\ \mu\text{m}$  and mineral-poor fuels rich in nanometre sized ( $<1\ \mu\text{m}$ ) PM (Table 1; Liati et al., 2012). The varied morphologies of the primary PM as a function of particle size are also dependent on the fuel type, and combustion conditions, such as temperature, PM cooling rates and combustion rates (Table 1; Liati et al., 2012; Vassilev & Menendez, 2005). Particle filtration systems fitted to coal burning plants since the 1970s, have modified the emitted size distinction between the emitted PM of the various fuel types, with a probable increasing importance of fly ash particles  $< 10\ \mu\text{m}$ , like in other fuel sources.

### **Mineral- rich fuels**

Inorganic PM in pulverised coal fly ash has been extensively investigated, since it is an industrial resource for various processes (e.g. cement manufacture), and poses a danger to groundwater contamination if buried in landfill. Increasingly, more is being understood about the inorganic PM produced from other fuel types, but its often nanometre size makes it difficult to study using many conventional methods, such as those applied to larger PM. Particle size is a fundamental control on the morphology of PM, and on magnetic behaviours (Fig. 1).

Coal fly ash is composed of a complex mix of particle morphologies, from relatively amorphous particles derived from the original fuel, through vesicular forms to a variety of spherical particles (spherules) produced by more complete exposure to the combustion process (Fig. 2; Vassilev & Menendez, 2005; Chen et al., 2005), and all transitions between these end-members. The content of opaque phases (Fe-oxides and carbonaceous phases) divides these particles into varying degrees of opacity (Fig. 2). Forms of spherule range from solid spheres (of silicates or oxides) to spherules that are hollow (cenospheres) to hollow spherules that are filled with smaller spheres called plerospheres (Fig. 2). Surfaces of the spherules (particularly the solid spherules) vary from smooth to being ornamented with a variety of crystals that range from small surface irregularities ('orange peel texture') to larger, well developed crystal growths (Vassilev & Menendez, 2005). This variety reflects mineralogical intergrowths within the spherules at a variety of scales from nanometre to several 10s of microns in size (Fig. 3i; Blaha et al., 2008). Spherules are more concentrated in the finer-micron-sized fractions of fly ash and other particles in the coarser fractions (Fig. 3), partly due to the fact the larger particles can be more carbon-rich, due to a higher concentration of non-combusted coal. The cenosphere content can vary widely from 5 to 95%, with coal ash content and moderate Fe contents favouring their formation. Average median mass grain size of fly ash is ca.  $10\ \mu\text{m}$ , with a range in median sizes from 2 to  $100\ \mu\text{m}$ , dependent on source. The finest particle fractions (i.e.  $< ca. 1\ \mu\text{m}$ ) of fly ash tend to be dominated by soot aggregates  $0.1\ \mu\text{m}$  to  $1\ \mu\text{m}$  in size (Figs. 3a,b), making them distinctively different from the  $>1\ \mu\text{m}$  fractions, and in this respect, these finest fractions are similar to PM from diesel engine emissions (Chen et al., 2005). Fe-oxide

particulates range down to nanometres sized particulates (Fig. 3k) and the <63  $\mu\text{m}$  fractions of coal fly ash dominate the magnetic properties (Blaha et al., 2008). PM size differences relate to the different formation processes, with larger particles produced by the coalescence and aggregation of molten metal-Si-phases, and the ultrafine-PM produced by vaporisation-condensation mechanisms (Fig. 1). Oil shale burning likely produces similar inorganic PM to coal-burning, but has not been so intensely studied.

### **Mineral-poor fuels**

PM from high temperature burning of wood and liquid fuels is dominated by carbonaceous PM, which tends to be composed of 20-30 nm sized primary carbon spheres which aggregate into larger soot particles (Fig. 3a, b, c). During mixing in the atmosphere, these may be combined with volatile PM of  $\text{NH}_4$  and Na sulphates and nitrates to produce complex secondary particles, the volatile components of which are removed under conventional vacuum and electron beam conditions when observed in SEM and TEM (Liati et al., 2012; Smith et al., 2012). Wood burning produces larger 30-40 nm primary carbon particles than those produced by vehicle engines. Low temperature wood burning tends to produce much larger amounts of carbonaceous spherules ('tar balls'; Fig. 3c) which range in size from 50- 600 nm in size. Diesel, petrol and heavy fuel oil combustion produce primary carbon particles of the order of 20-50 nm in size. Aggregated carbon particles dominate the mass distribution of these fuel types, with most of this mass is concentrated in the ca. 0.1 to 1.5  $\mu\text{m}$  size range.

The inorganic PM produced by wood and liquid fuels is highly varied and strongly depends on the trace element composition of the raw fuel and any fuel additives (Liati et al., 2012; Sanderson et al., 2014). These fuel types produce only small amounts of inorganic spherules, and compound intergrowths with nanometre sized spherules of carbon (Figs. 3d,e,f, g). In diesel engines under high loads or with larger amounts of fuel additives, metal oxides may act as cores for peripheral carbon deposition (Fig. 3g). The main mass of the inorganic PM tend to be composed of irregular and crystalline shaped particles intimately associated with the carbonaceous PM, and of a similar particle size to the aggregated carbon PM (Fig. 3; Liati et al. 2012; Smith et al., 2012).

### **Magnetic characterisation**

As a result of the relatively high concentrations of the Fe-oxides magnetite and haematite in fly ash, magnetic measurements are particularly simple to use as a proxy for the total Fe-load of the inorganic PM (Locke and Bertine, 1986; Mclean, 1971). Historically in developed countries, heavy loads of fly ash were deposited in soils, lakes and peat and can be easily identified as such (Oldfield et al., 2015). Magnetic measurements such as magnetic susceptibility ( $\chi_{\text{LF}}$ ) and remanence measurements of saturation isothermal remanent magnetisation (SIRM), anhysteretic remanent magnetisations (ARM, expressed as  $\chi_{\text{ARM}}$ ) or high-field IRM (HIRM, that produced at magnetic fields > 0.3 T) provide simple proxies for the total Fe-oxide load. SIRM at magnetic fields >0.5 T respond to the total Fe-oxide load,  $\chi_{\text{ARM}}$  is most sensitive to magnetite particulates around 0.03  $\mu\text{m}$  in size and HIRM to the concentration of haematite (or goethite).

However, at low pollution PM loads the intrinsic magnetic properties of natural dusts, soils and sediments can mask this magnetic relationship (Snowball et al., 2014). For this reason the first magnetic measurements of pollution-related PM were established in peat cores, which is intrinsically nearly non-magnetic due to low concentrations of natural particles (Oldfield et al., 2015). For much

the same reason organic-based PM collectors such as tree or plant leaves, tree bark, moss and lichen have proven popular for magnetic studies of spatial distribution of PM pollution and changes in medium and short-term PM pollution loads, since the collector material for the PM can largely be ignored (Petrovsky & Ellwood, 1999; Bourliva et al., 2016), circumventing collector and PM physical separation.

### **Mineralogy and chemistry**

Coal fly ash is dominated by amorphous phases of silicate glass and char, comprising roughly 40 to 80% of its mass. The main crystalline components in fly ash are Mullite ( $2 \text{Al}_2\text{O}_3 \cdot \text{SiO}_2$ ), quartz ( $\text{SiO}_2$ ), feldspars, magnetite ( $\text{Fe}_3\text{O}_4$ ), haematite ( $\text{Fe}_2\text{O}_3$ ), lime (CaO) and anhydrite ( $\text{CaSO}_4$ ), along with some 316 known accessory mineral phases. The chemistry of the inorganic component in fly ash broadly follows similar trends to the average crustal abundance in rocks, which reflects the inorganic contamination in coals (Fig. 5a). However, there is much variation between fly ashes due to variation in the inorganic chemistry of the source coals. The inorganic PM fractions of fly ash below  $0.1 \mu\text{m}$  have a chemistry (containing Fe-Ti-Al oxides, or phosphates, silicates and sulphates) related to fuel sources, but distinctly different particle morphologies to the larger-sized fractions (Chen et al. 2005).

The inorganic mineral content of PM from mineral-poor liquid fuels such as diesels and petrol (kerosene) is complex and incompletely understood, since it depends on combustion conditions, interactions with filtration systems and the nature of fuel additives. This is confounded by the often nanometre size of the particulates, and the advanced methods of microscopy and analysis required to study them (Liati et al., 2012; Sanderson et al., 2014).

Metal elements in diesel ash (fuel oil and vehicles; Table 2; Fig. 5b) tend to be dominated by Ca, Mg, P, Zn, Fe, Ni and V principally in the form of: a) sulphates such as Ca-Na-OH sulphates,  $\text{CaSO}_4$  and Fe-Ni sulphates, which may be variably hydrated; b) sulphides such as CaS and NiS; c) Phosphates such as  $\text{ZnMgPO}_4$ ; d) oxides of metal elements such as CaO,  $\text{V}_2\text{O}_5$  or  $\text{NiAl}_2\text{O}_4$ , spinel-type oxides of Fe-Ni-V-Zn (close to magnetite in structure), and haematite ( $\text{Fe}_2\text{O}_3$ ); e) Metallic Fe-Cr±Ni and f) silicates both as glassy spherules and crystalline Mg-Al-silicates. These phases are often between a few nm in diameter to  $\sim 200 \text{ nm}$  often intimately mixed and intergrown with the much larger concentrations of soot and char. Fe-based fuel additives have a large influence on the concentration of Fe-minerals, and the relative concentration of Fe-minerals increases with decreases in the carbon emitted. Petrol-based emissions probably produce similar particulates.

Sulphates, sulphides and metallic elements are particularly subject to secondary modification once emitted into the air to generate secondary oxides (and also modified during burial in soils and sediments). This is probably seen by the few studies which have examined the Fe-phases from vehicle emissions in urban areas, which have largely identified magnetite as the primary Fe-oxide, but which in primary engine emissions seems to be a minor phase (Smith et al., 2012). Magnetic measurements at low temperatures and variable frequencies have indicated that ambient air-borne Fe-oxides can have high abundances of superparamagnetic magnetite particle  $< 30 \text{ nm}$  in size, which may also be a reflection of the secondary modification of compound Fe-soot particles. An unresolved conundrum is that many magnetic-based studies of vehicle pollution conclude the magnetic signal is associated with spherules, which are not abundant in studies of vehicle engine emissions. It is not clear if this is due to ambient contamination from fly ash sources, 'secondary ageing' of nm-sized Fe-particulates on carbonaceous spherules to produce highly magnetic compound magnetite-char

spherules or underrepresentation of the nanometre-sized Fe-oxide particulates in microscopy. Alternatively, and perhaps most likely, it may relate to the sensitivity of the magnetic method to these minor spherule components produced in liquid-fuel combustion.

Wood-ash inorganic PM is dominated by K, Cl, S, Zn, Si and the inorganic PM concentration emitted in wood and pellet burners are directly related to the concentration in the fuel. The major minerals produced are various kinds of K-Cl sulphates and carbonates along with ZnO (Figs. 4h, I, j). Under some burning conditions the coarse component can be dominated by carbonaceous spherules. Fe is a minor to trace component in wood-burning PM (Table 1), so it appears magnetic signatures from wood burning are minimal, but magnetic studies evaluating this potential source are sparse.

### **Magnetic fingerprints for fuel burning**

Magnetic measurements that generate SIRM and  $\chi_{\text{ARM}}$  values have provided suitable proxies for monitoring spatial and time-variations in anthropogenic pollution (Locke & Bertine, 1986; Petrovsky & Ellwood, 1999). This is primarily related to the fact that anthropogenic PM tends to be richer in Fe-oxides than many natural dusts that have been studied (Fig. 6), leading to larger values of  $\chi_{\text{LF}}$ , SIRM and  $\chi_{\text{ARM}}$  which large express iron oxide concentration (Fig. 6). For example in primary emissions  $\chi_{\text{LF}}$  is most often  $>900 \times 10^{-8} \text{ m}^3 \text{ Kg}^{-1}$ , whereas large proportions of natural dusts seem to have  $\chi_{\text{LF}}$  most often  $<200 \times 10^{-8} \text{ m}^3 \text{ Kg}^{-1}$ . The exceptions to this seem to natural dusts with Fe-oxide contents derived from magnetically enhanced soils, which are richer in ultra-fine grained magnetite (Figs. 6, 7). Although magnetic data on primary anthropogenic fuel emissions and natural dusts is incomplete, similar relationships may hold for SIRM and  $\chi_{\text{ARM}}$  (Fig. 6).

Compared to the data available for natural dusts, urban, largely vehicle-derived dusts seem to be magnetically dominated by rather coarse magnetite particle fractions, as evident by the low  $\chi_{\text{LF}}$ /SIRM and  $\chi_{\text{ARM}}$ /SIRM ratios which express proxies for magnetite particle size (Fig. 7). It is not clear why this is, since magnetite PM seen in microscopy is often intimately mixed with silicates in sub-micron textures, implying ultrafine magnetic particle sizes may be important (Blahe et al., 2008). Also, some studies on urban dusts have estimated 63-75% of the magnetic load at 15K to be carried by magnetite particles  $<17 \text{ nm}$  in size. It may be that high temperature formation of the pollution PM Fe-oxides has rather defect free magnetite, compared to geologically natural magnetite, which typically has more complex low temperature origins in surface sediments and soils.

Magnetic studies have often sought to explore relationships between magnetic mineral concentrations (expressed by  $\chi_{\text{LF}}$ , etc) and chemical concentrations, in the expectation that both covary with pollution PM loads. Most such studies have taken place with respect to modern urban-vehicle derived PM. However, these relationships vary considerably between studies and study sites due to the complexity in the mix of sources, particle collector systems and the multi-sourced anthropogenic origins of many elements (Table 2). Most studies show scattered but often linear positive relationship between magnetic data and heavy metal content, perhaps best expressed by Fe, Zn, Cu and perhaps Co (Fig. 8). Zn and Co are often associated with tyre and brake wear and Cu with brake wear and diesel engine PM emissions (Table 2). Zn and Cu are also much enhanced in urban environments compared to typical rock values (Fig. 4b). Fe has many sources (Table 2) but is depleted in primary engine emission PM compared to that in natural PM loads (Fig. 5b), suggesting Fe may be derived principally from road or vehicle wear and tear. The few studies which have explored relationships of magnetic mineral concentration and nitrous oxide and polycyclic aromatic

hydrocarbon emissions generally show strong positive relationships (Fig. 8), whereas that with  $PM_{10}$  load is not universally good. This is probably related to the low contents of particles  $> 10 \mu m$  in some urban dusts and the variable amounts of Fe in this size fraction (Sanderson et al. 2014; Bourliva et al. 2016).

### Timing of fossil fuel burning as seen in magnetic data

The mineral magnetic record of atmospheric PM pollution related to fossil fuel burning has left behind a strong record of magnetic Fe-oxides in peat bogs and lakes (Oldfield et al., 2015), largely due to industry-related coal burning which started during the industrial revolution. This was first clearly demonstrated in peat bogs (since other contaminating minerals and dusts were largely absent), and later demonstrated in lake sediments (Locke and Bertine, 1986; Oldfield, 1990). The magnetic response is one that is nearly always displayed as an increase in Fe-oxide abundance expressed by  $\chi_{LF}$ , SIRM and sometimes HIRM (Snowball et al., 2014). These abundance increases relate to both magnetite (expressed by  $IRM_{0.2T}$ ; Fig. 9c) and hematite (expressed by HIRM; Fig. 9b) or both these minerals (SIRM). The relationship to coal-burning PM loads is largely through an association with approximate timing of fuel burning (right panel in Fig. 9a), in parallel with increases in heavy metal loads in the peat and sediment cores. Only few magnetic-based studies have directly observed the association to coal fly ash spherules, as often inferred (Locke and Bertine, 1986; McLean 1991). Interpreted increases in magnetic mineral abundance are also seen in some coastal and marine sediments, where they are also associated with increases in heavy metal concentrations. The magnetic record of pollution PM in lakes and bogs is largely from relatively few studies in Britain, Scandinavia and North America, but is expanding with more studies in SE Asia.

The earliest substantial evidence in the magnetic records for fly ash loads is around AD 1800 in the peat bogs of northern England (Oldfield et al., 2015) and New Brunswick in Canada (Fig. 9b). These timings concur with the first occurrence of carbonaceous spherules (Rose, 2015). The initial increases in the magnetic data seem to be associated with developments in the industrial uses of coal (for steel making etc), rather than domestic and industrial heating. In London coal was the most important source of heating for domestic and industrial use from the mid 17<sup>th</sup> century, and even by AD 1800 many British cities were extremely smoky and polluted. Yet the widespread expression of this domestic use did not produce major export of fly-ash, magnetic signatures or carbonaceous spherules (Rose, 2015). In locations remote from urban centres (such as the Scottish Highlands; Fig. 9a) the export of coal-based PM from urban and industrial sites was clearly delayed until later (Fig. 9a; Snowball et al. 2014). Reasons for this are not entirely clear, but may be related to expansion in the industrial use of pulverised coal combustion, burning at higher temperatures and more effective and taller chimneys allowing greater dispersal of PM after AD 1900. Ombrotrophic peat records seem to show the increase in magnetic PM loads to start ca 50 years before lake records (Oldfield et al., 2015), which in the lake sediments may be a reflection of the initially small magnetic PM inputs being swamped by lake detrital inputs.

Localised 16<sup>th</sup> and 17<sup>th</sup> century magnetic evidence for pollution PM also occurs in northern England and southern Scotland, probably associated with charcoal-based metal smelting (Oldfield et al. 2015). The largest number of studied sites containing major initial increases in these inferred magnetic pollution particulates probably dates around AD 1900 (Fig. 9a, c), when there was more rapid regional increases (Oldfield et al., 2015). Quantitative estimates of magnetic particulate accumulation rates have rarely been made, so we have much to learn about how to use the

magnetic data, before their links to urban and rural PM loads and sources can be understood in the Anthropocene. The more direct approach using carbonaceous spherules, with a much larger dataset than available to magnetic studies, suggests globally major growth in coal burning did not take place until after ca. 1950 (Rose, 2015), when major industrial expansion took place in eastern Asia. This expansion in magnetic PM loads in the 1950s is seen in the few magnetic records we have from SE Asia, Africa and South America (Snowball et al., 2014). {3397 words}

## References

- Blaha, U., Sapkota, B., Appel, E., Stanjek, H. & Rösler, W. (2008). Micro-scale grain-size analysis and magnetic properties of coal-fired power plant fly ash and its relevance for environmental magnetic pollution studies. *Atmospheric Environment*, **42**, 8359-8370.
- Bourliva, A., Papadopoulou, L. & Aidona, E. (2016). Study of road dust magnetic phases as the main carrier of potentially harmful trace elements. *Science of the Total Environment*, **553**, 380-391.
- Chen, Y., Shah, N., Huggins, F. E. & Huffman, G. P. (2005). Transmission electron microscopy investigation of ultrafine coal fly ash particles. *Environmental Science & Technology*, **39**, 1144-1151.
- Gieré, R. & Querol, X. (2010). Solid particulate matter in the atmosphere. *Elements*, **6**, 215-222.
- Liati, A., Eggenschwiler, P. D., Gubler, E. M., Schreiber, D., & Aguirre, M. (2012). Investigation of diesel ash particulate matter: a scanning electron microscope and transmission electron microscope study. *Atmospheric Environment*, **49**, 391-402.
- Locke, G. & Bertine, K.K. (1986). Magnetic sediments as an indicator of coal combustion. *Applied Geochemistry*, **1**, 345-356.
- Mclean, D. (1991). Magnetic spherules in recent lake sediments. *Hydrobiologica*, **214**, 91-97.
- Oldfield, F. (1990). Magnetic measurements of recent sediments from Big Moose Lake, Adirondack Mountains, N.Y., USA. *Journal of Paleolimnology*, **4**, 93-101.
- Oldfield, F., Gedye, S. A., Hunt, A., Jones, J. M., Jones, M. D. & Richardson, N. (2015). The magnetic record of inorganic fly ash deposition in lake sediments and ombrotrophic peats. *The Holocene*, **25**, 215-225.
- Petrovsky, E. & Ellwood., B.B. (1999). Magnetic monitoring of air- land and water pollution. In: Maher, B.A. & Thompson, R. (eds.) *Quaternary climates, environments, and magnetism*. Cambridge: Cambridge University Press, p. 278-322.
- Rose, N. L. (2015). Spheroidal carbonaceous fly ash particles provide a globally synchronous stratigraphic marker for the Anthropocene. *Environmental Science & Technology*, **49**, 4155-4162.
- Sanderson, P., Delgado-Saborit, J. M. & Harrison, R. M. (2014). A review of chemical and physical characterisation of atmospheric metallic nanoparticles. *Atmospheric Environment*, **94**, 353-365.
- Smith, S., Ward, M., Lin, R., Brydson, R., Dall'Osto, M. & Harrison, R. M. (2012). Comparative study of single particle characterisation by Transmission Electron Microscopy and time-of-flight aerosol mass spectrometry in the London atmosphere. *Atmospheric Environment*, **62**, 400-407.
- Snowball, I., Hounslow, M. W. & Nilsson, A. (2014). Geomagnetic and mineral magnetic characterization of the Anthropocene. In: Waters, C. N., Zalasiewicz, J. A., Williams, M., Ellis,

M. A. & Snelling, A. M. (eds). *A stratigraphical basis for the Anthropocene*. Geological Society, London, Special Publications, 395, 119-141.

Vassilev, S. V. & Menendez, R. (2005). Phase-mineral and chemical composition of coal fly ashes as a basis for their multicomponent utilization. 4. Characterization of heavy concentrates and improved fly ash residues. *Fuel*, **84**, 973-991.

## Figure captions

Fig. 1. Typical particle sizes (i.e. equivalent spherical diameter) and abundances of anthropogenic particles in urban settings (blue curve), road-sides (grey dashed), coal fly ash (red curve) and natural terrestrial dusts (green curve). All curves except fly ash in volume of particles per  $\text{cm}^3$ . The fly ash curve is the relative volume, in which the area under the curve sums to 100%. Area under other curves will sum to the total PM volume per  $\text{cm}^3$ . Aerosol size (mode) categories shown and magnetic particle behaviour in magnetite equivalent cubic size. Superparamagnetic magnetite does not carry a remanence at room temperature, unlike larger sized particles. Dotted lines in single domain field are transition intervals into the finer and coarser thresholds, dependent on degree of particle interaction.

Fig. 2. Morphological variety of particulates found in fly ash from coal combustion, based on their opaque content. Opaque materials may be carbonaceous or Fe-oxide bearing. Spherules may be silicate (glass plus crystalline components), Fe-oxide (magnetite and haematite) or carbon based, and take on three spherical forms aperture-rich hollow spherical shells (cenospheres), solid, or cenospheres filled with smaller spherules (plerospheres). See Vassilev & Menendez (2005) for details. Large particle size amorphous material may represent unburnt fuel, whereas smaller sized amorphous material has more complex origins related to the ultrafine-grained soot of fly ash (Chen et al., 2005). Silicate glass spherules varies in colour from white to near opaque due to varying amounts of included sub-micron Fe-oxides.

Fig. 3. Typical morphological variety of fly ash as an approximate function of particle size from a US power plant. The particle-sized fractions represent fractions collected by cyclone separators, and median sizes is the size obtained by Stokes Law sedimentation analysis. Values in [...] are median particle sizes determined by electron microscopy, and are different to sedimentation sizes due to particles during sedimentation aggregating. Labels on columns are: T= Transparent, M=Mixed, O= Opaque components, C=cenospheres, P=plerosphere and S=solid spherules as in Fig. 2.

Fig. 4. Morphological variety of nanometer-sized particles derived from fuel sources. a), b) typical soot aggregates composed of chain-like collections of ca. 20 nm sized carbon particles, observed in transmission electron microscope (TEM), with TEM support grid arrowed in a). c) Carbonaceous spherules (or tar balls) in TEM. d) Ca-Mg rich particles in irregular and spherical form from oil-shale burning, observed in TEM. e). f) Relatively large irregular Fe-rich particles in e) and a large rectangular Si-Ti crystal in f), observed in a scanning electron microscope. g) and h) FeO and ZnO as cores to carbon nanoparticles respectively, observed in TEM. i) compound spherical char particle with inorganic material internally, TEM. j) Primary  $\text{K}_2\text{SO}_4$  and ZnO particles observed in TEM. k) Iron-oxide nanoparticles attached to the surface of a large aluminosilicate particle in the ultra-fine



fraction in a Kentucky coal fly ash. Fuels sources: automobile diesel engine soot- b), c), d), g and h) ; heavy fuel oil in ships diesel engine- e), f), i) ; wood burning soot - a), j).

Fig. 5. Selected element chemistry of PM from solid and liquid fuels. Those in a) are solid primary coal fuel sources. Those in b) are the limited data from primary diesel sources and the more abundant data from road dusts, which are a mix of primarily engine emission particulates, with tyre, breaks and road wear and tear, mixed with smaller amounts of other sources. Red arrows adjacent to Fe indicate typical range in Fe-contents in rocks. The MRG-1 rock standard is a gabbro.

Fig. 6. Summary magnetic mineral abundance data for PM from; a) anthropogenic sources and b) natural PM dust sources. The three magnetic proxies ( $\chi_{LF}$ , SIRM and  $\chi_{ARM}$ ) respond differently to differing mixes of magnetic minerals and magnetic particle sizes. SIRM responds to both magnetite and hematite in all particle sizes greater than ca. 0.03  $\mu\text{m}$  whereas  $\chi_{ARM}$  responds most strongly to magnetite particle sizes ca. 0.03  $\mu\text{m}$ .  $\chi_{LF}$  responds in addition to superparamagnetic (magnetite particles less than ca. 0.02  $\mu\text{m}$ ) and paramagnetic (e.g. Fe-silicate) particles. Broadly, primary anthropogenic PM sources have  $\chi_{LF}$  and SIRM greater than ca.  $900 \times 10^{-9} \text{ m}^3 \text{ kg}^{-1}$  and ca.  $10,000 \times 10^{-5} \text{ Am}^2 \text{ kg}^{-1}$  respectively, although there are few magnetic studies on PM generated by primary fuel emissions. The Beijing subway samples may be so strong due to metal Fe or FeO particulates. Labels on natural dust sources are, P= primary fuel PM studies. O= oceanic aerosols, T=terrestrial dusts.

Fig. 7. Bi-plot of magnetic proxies that express magnetic particle size for magnetite. Anthropogenic PM (predominantly from traffic-generated PM studies) tends to be distinctly coarser in these magnetic particle-size proxies than most natural dusts, as shown by the smaller values of these two proxies. Although there are limited data, indoor dusts tend to have larger  $\chi_{LF}$ /SIRM ratios than outdoor dusts for reasons that are not clear. There are no comparable data for PM from primary fuel types. Note that magnetic particle size does not necessarily relate directly to physical size (e.g. like in Fig. 1) since natural magnetite particles are normally sub-divided into smaller regions by non-magnetic intergrowths.

Fig. 8. Summary of the strength of linear correlation (expressed by Pearson R coefficient) between PM chemistry and  $\chi_{LF}$ . This data is derived entirely for vehicle-related PM. Similar studies on other sources of PM and other magnetic parameters are sparse. PAH= polycyclic aromatic hydrocarbons.

Fig. 9. Example magnetic datasets that show response of magnetic –mineral abundance variables to the generally increasing coal fly ash loads since around AD 1800. A) Lake sediment cores from rural Scottish (Loch Nah Achlaise and Lochnager) and Welsh (Llyn Dulyn) lakes (from Oldfield et al., 2015), and British energy consumption in Tonnes of coal equivalent (Tce). b) Regent Street Bog, New Brunswick, Canada (blue curves); Big Moose lake, Adirondack, NY State, USA (red curves) (Oldfield, 1990). C) Three small lakes in NE Pennsylvania, which show increase in magnetic PM loads from AD 1900 and a reduction in loads since the 1970s, when PM filters were fitted to power stations.

Table 1. Grain size characteristics and simple characteristics of PM produced by fuel types, as weight % values. (..) show the range of weight % for a variety of fuel sources. Approximate magnetic fraction for wood, peat, diesel and petrol is based on SIRM of ash using the saturation remanence for magnetite. Excludes water and unburnt fluids in diesel/engine data. Magnetic fraction in heating oil and steel plants based on Fe content, so is a maximum. Data mostly prior to cleaning and particulate separators. [..]<sup>+</sup> the benzene soluble fraction.

| <b>Fuel /source Type</b> | <b>% &lt;0.1 μm</b> | <b>% &lt; 1μm</b> | <b>%&lt;10μm</b> | <b>%&lt;63 μm</b> | <b>%Water Soluble fraction</b> | <b>%Magnetic fraction</b> | <b>%Carbon</b> |
|--------------------------|---------------------|-------------------|------------------|-------------------|--------------------------------|---------------------------|----------------|
| Pulverised coal          | <5 (0,10)           | 2 (0,5)           | 25(5,50)         | 70 (38, 99)       | 1.6 (0.2, 7.2)                 | 8 (1, 20)                 | 3.1 (0.6, 9.8) |
| Steel plant              | <1                  | 10                | (30-95)          | 100               | ?                              | 1.7-13                    | 10 (4-16)      |
| Diesel/Petrol engines    | ~15                 | ~ 90              | (95,100)         | 100               | ~1 [10-90] <sup>+</sup>        | 0.1-0.2                   | 90 (76-99)     |
| Fuel oil (domestic heat) | ~20                 | ~50               | (90-95)          | 100               | ?                              | <1%                       | ~70            |
| Wood                     | ~15                 | ~90               | 95               | 100               | ~ 10-30                        | <0.5 (0.1, 0.9)           | ~ 35           |
| Peat                     | ~ 15                | ~ 90              | 95?              | 100               | ~ 10-30                        | <1% (0.3, 1.0)            | ?              |

Table 2. Metals in ultrafine particles associated with known urban and industrial sources. Those marked in bold are associated with high and generally consistent correlations with  $\chi_{LF}$  in Fig. 8.

| <b>Source type</b>                 | <b>Associated elements</b>                   |
|------------------------------------|--|
| Diesel                             | Al, Ca, <b>Cu, Fe</b> , Mg, Mn, V, <b>Zn</b> |
| Gasoline (emissions)               | Sr, <b>Cu</b> , Mn                           |
| Lubricating oil                    | <b>Fe</b> , Ca, P, <b>Zn</b> , Mg            |
| Fuel-borne catalysts               | <b>Fe</b> , Mn, Ce                           |
| Diesel fuel (marine engines)       | Al, Ca, <b>Fe</b> , Ni, V, <b>Zn</b>         |
| <b>Non-exhaust traffic sources</b> |  |
| Brakes                             | <b>Fe, Cu</b> , Sn, Zn                       |
| Tyres                              | Cd, <b>Co</b> , Cr, <b>Cu, Fe</b> , Mn, Pb   |
| Road dust                          | Zn, Al, K, <b>Fe</b> , Na, Mn                |
| <b>Industrial sources</b>          |  |
| Metalworking                       | <b>Fe</b> , K, Na, Pb, <b>Zn</b>             |
| Power generation                   | Ce, <b>Fe</b> , La, Na, K, V,                |
| Incinerators                       | Cd, Pb, Sb, <b>Zn</b>                        |

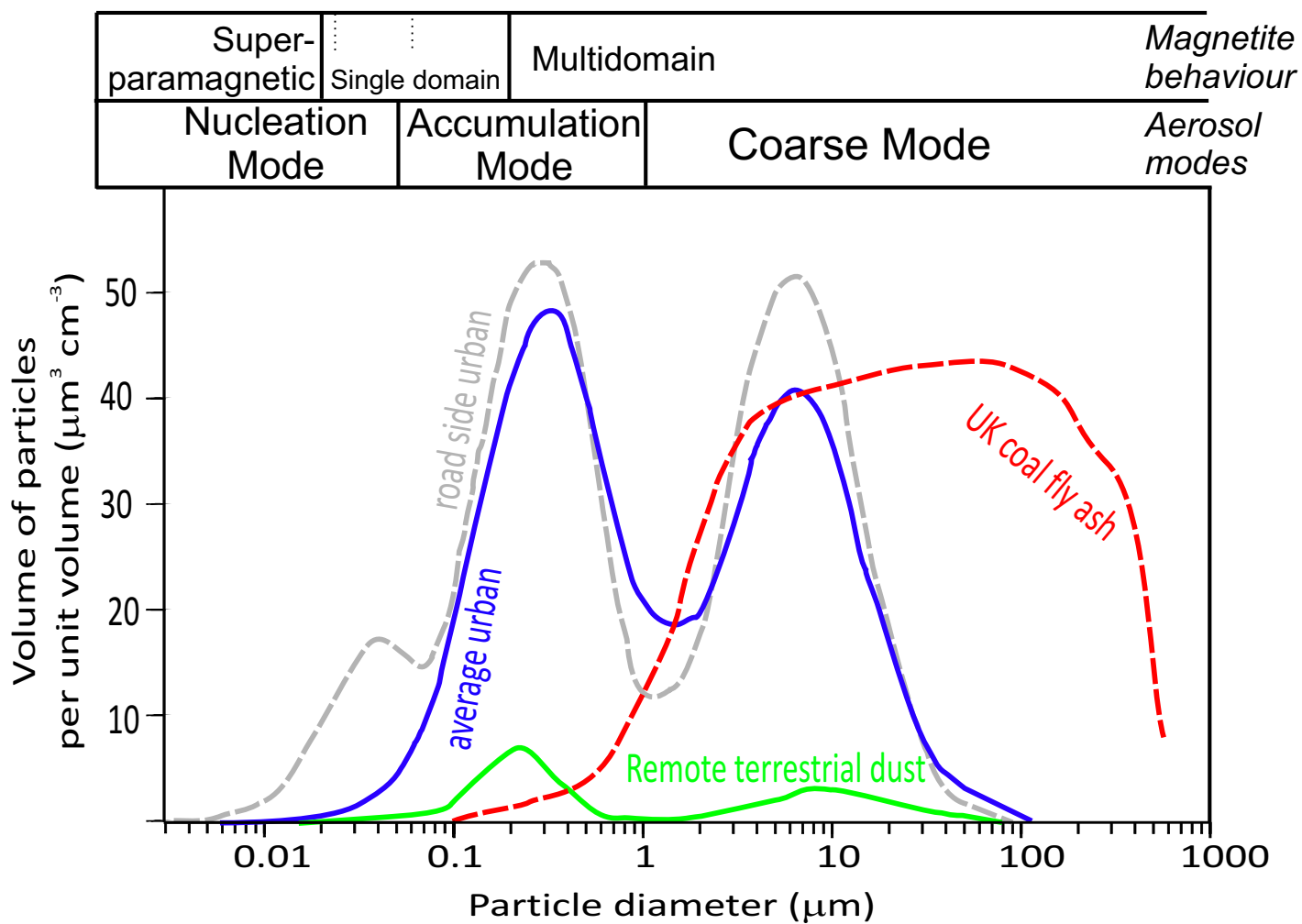


Fig. 1

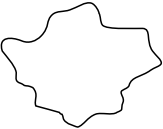
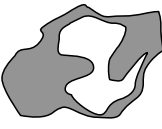

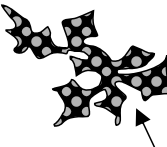
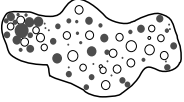
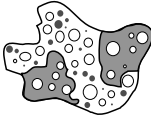
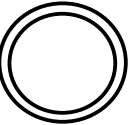
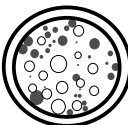
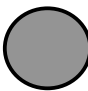

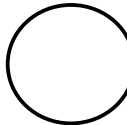
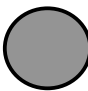
| Shape                     | Opacity   |  |  |
|---------------------------|---|--|--|
|                           | Transparent   | Mixed  | Opaque   |
| Amorphous                 | <br>Silicates  | <br>Silicates, coal & Fe-oxides | <br>Coal or Fe-oxides   |
| Lacy                      |   |  | <br>Carbonaceous  |
| Rounded vesicular         |                |                                 |  |
| Spherules<br>(± crystals) | <br>Cenosphere | <br>Plerosphere                 | <br>Fe oxides<br><br>Carbonaceous |
|                           | <br>Solid      | <br>Solid                      |  |

Fig. 2

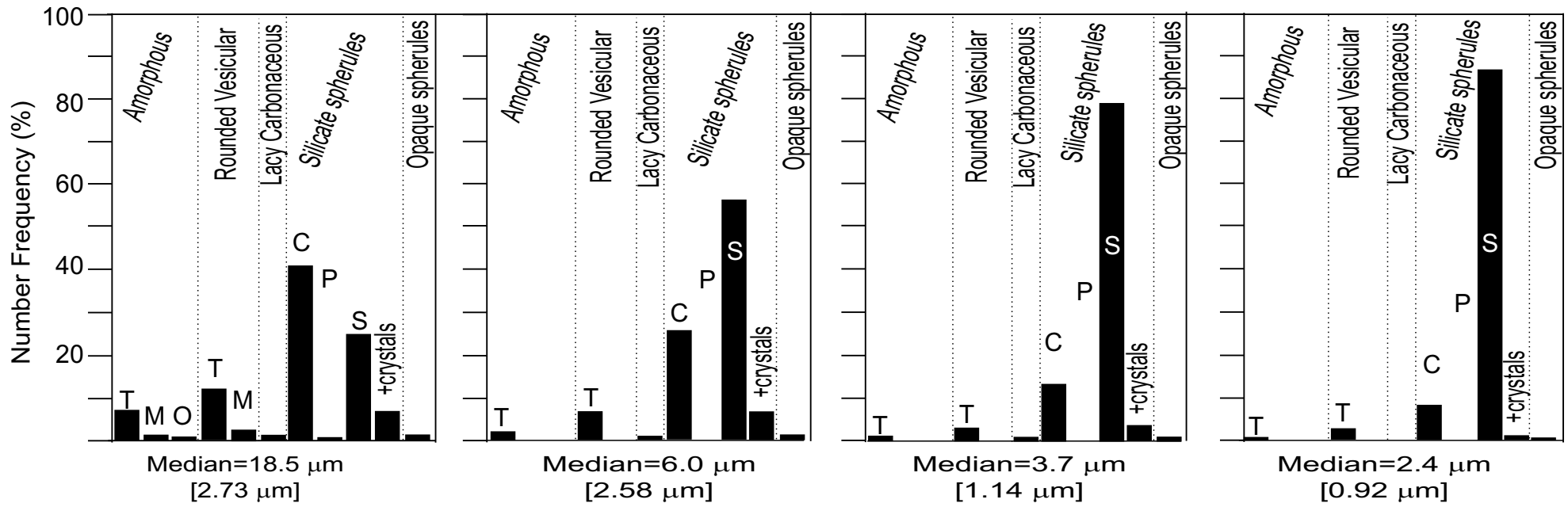


Fig. 3

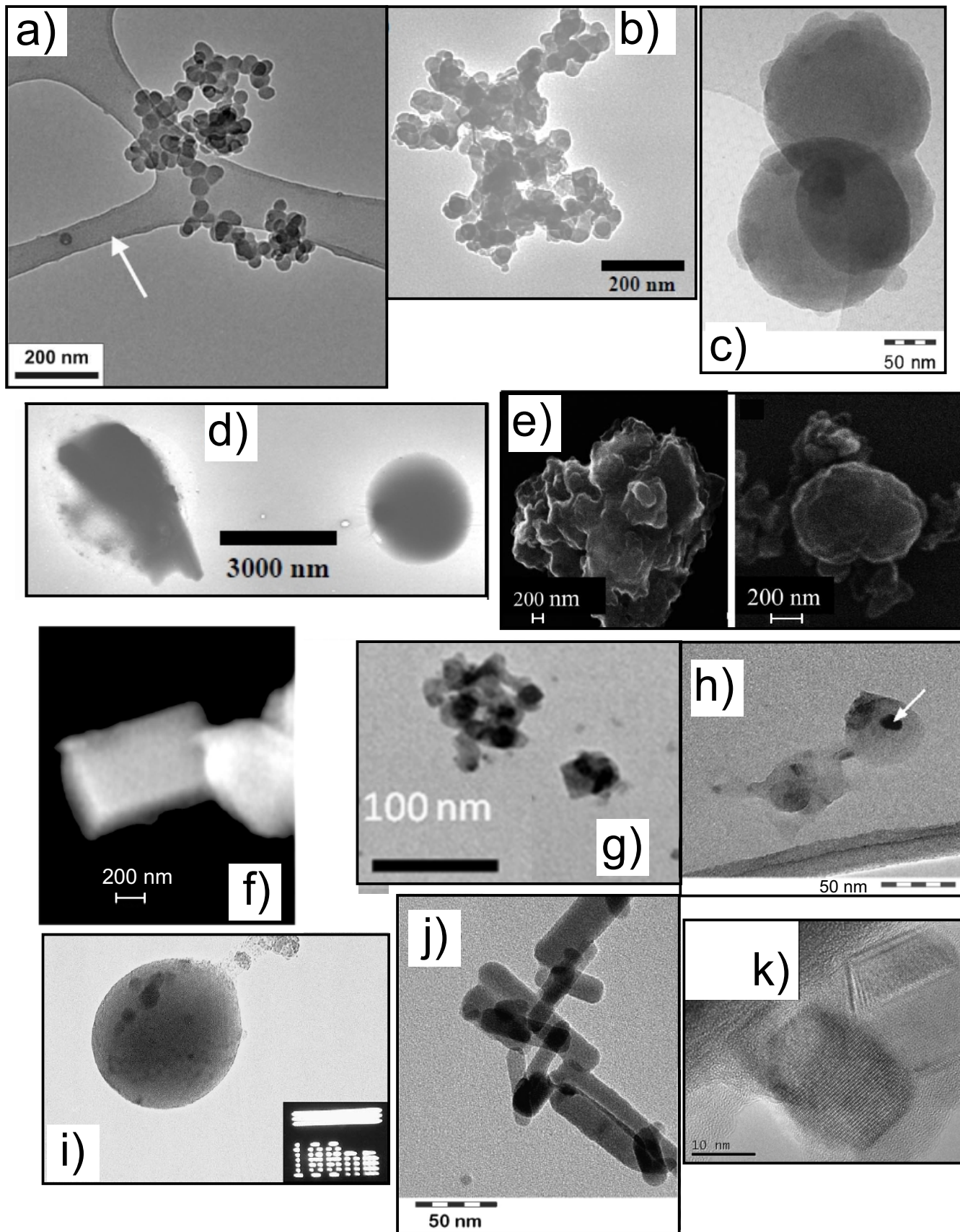


Fig. 4

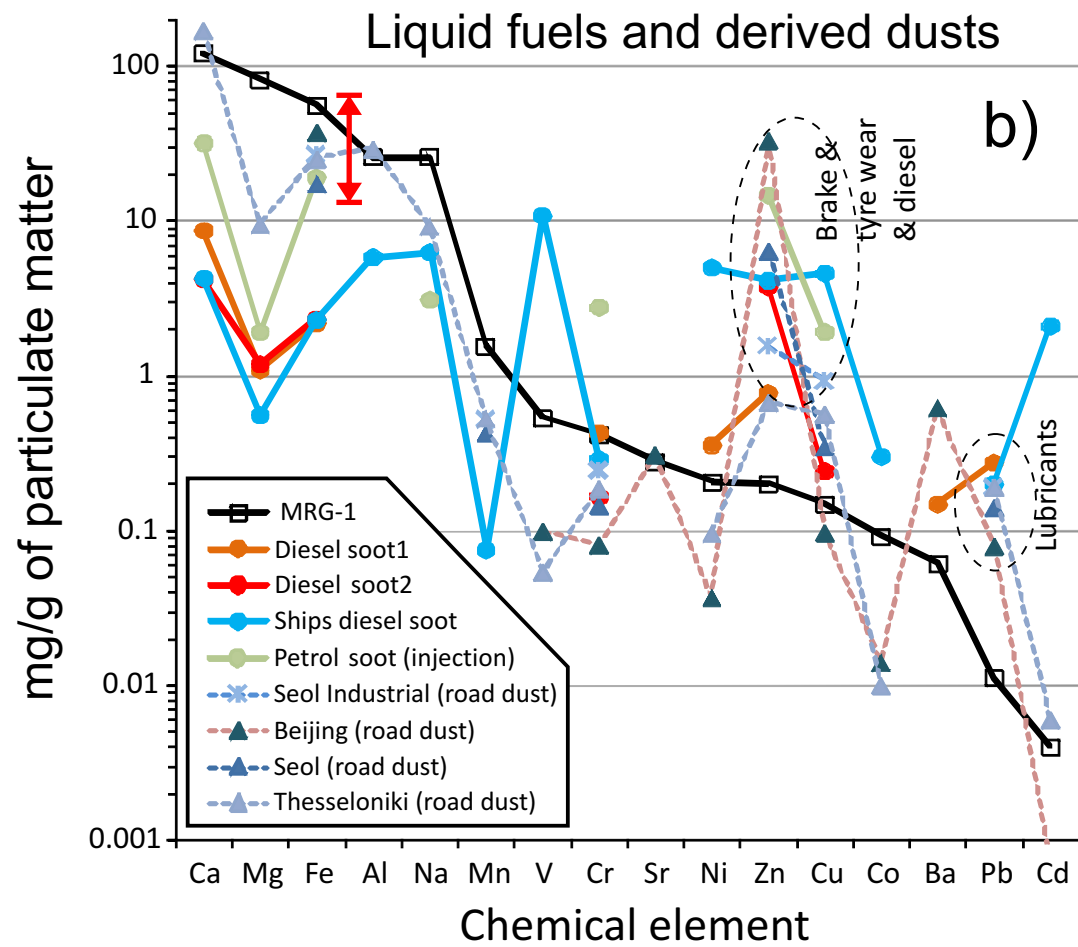
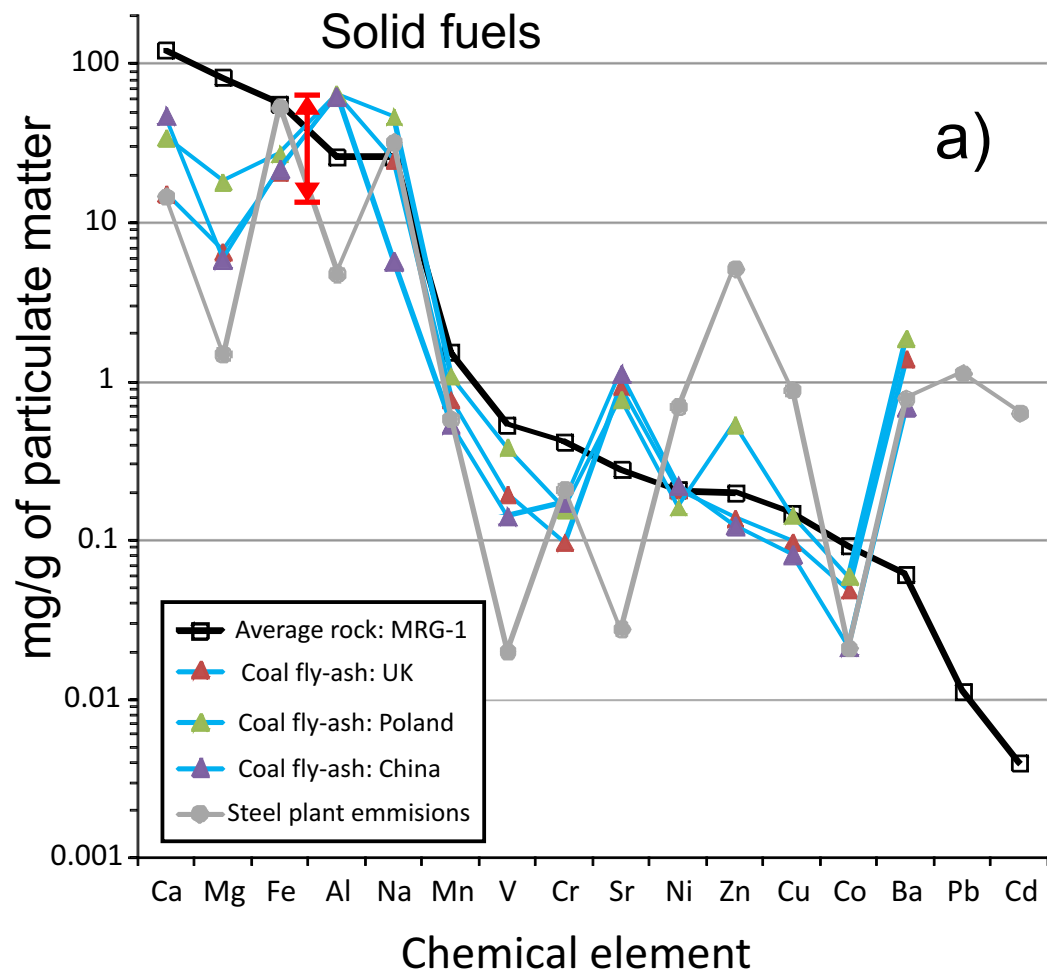


Fig. 5



a) Anthropogenic dust sources

b) Natural dust sources

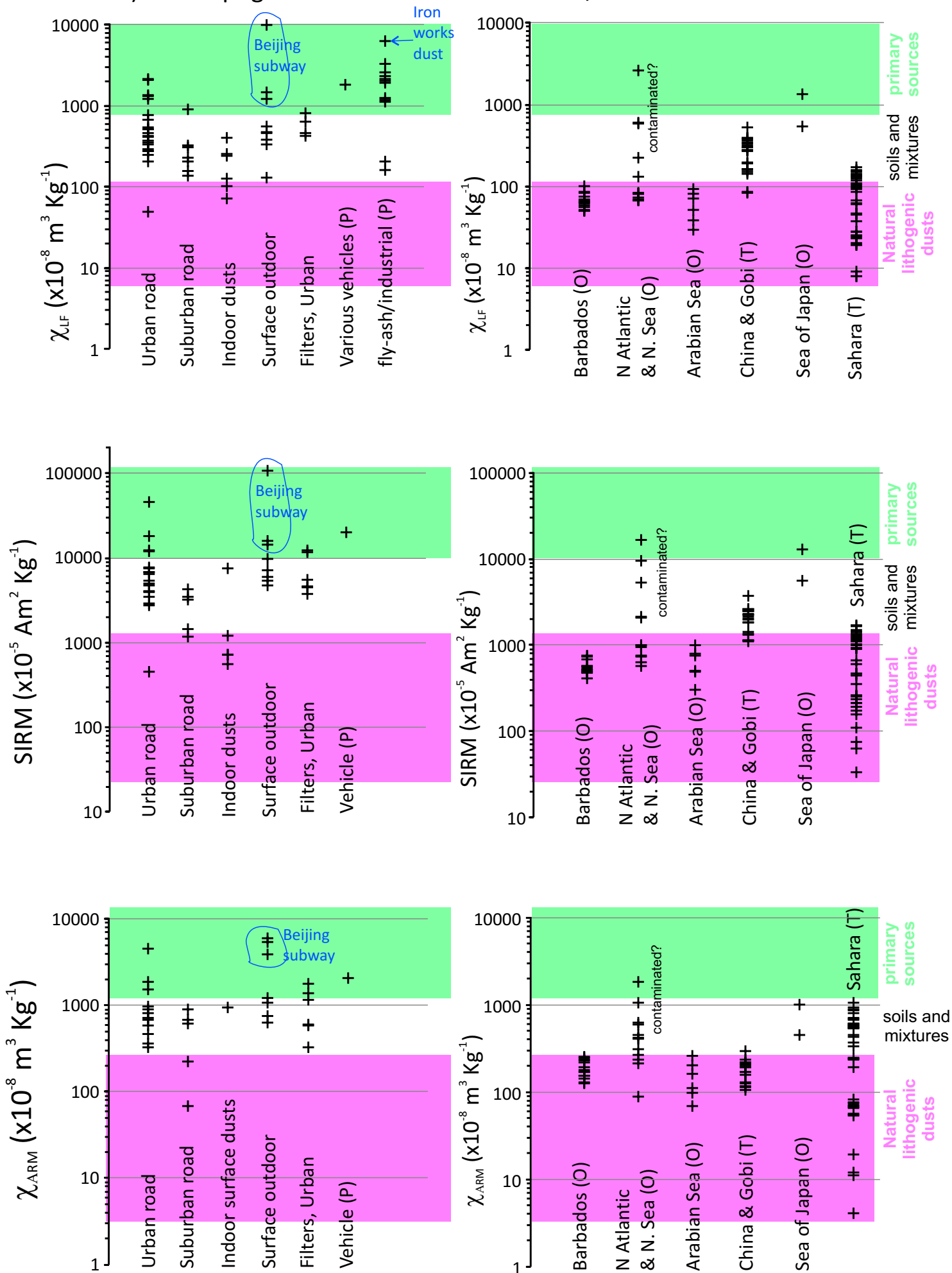


Fig. 6

Fig. 7

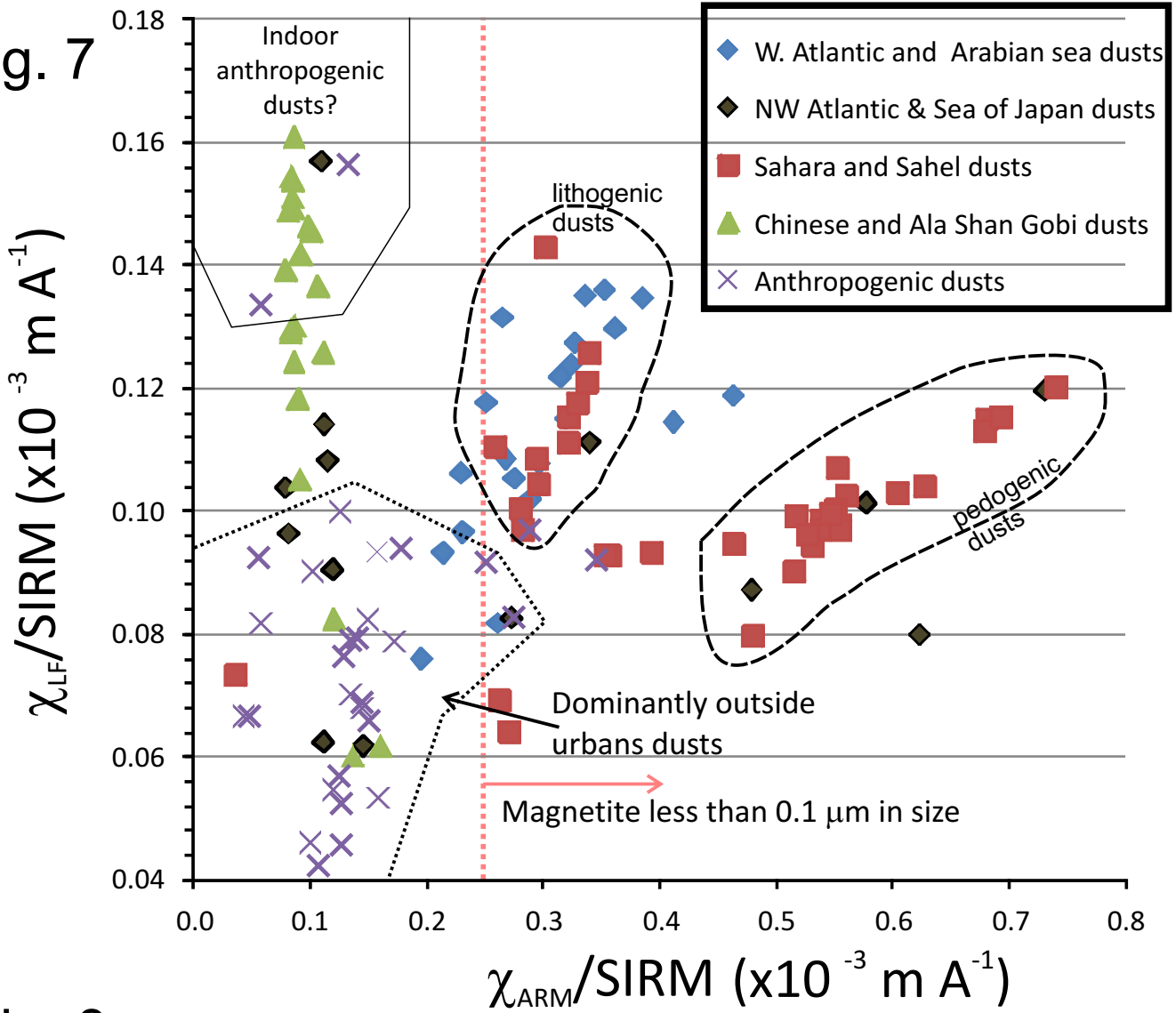
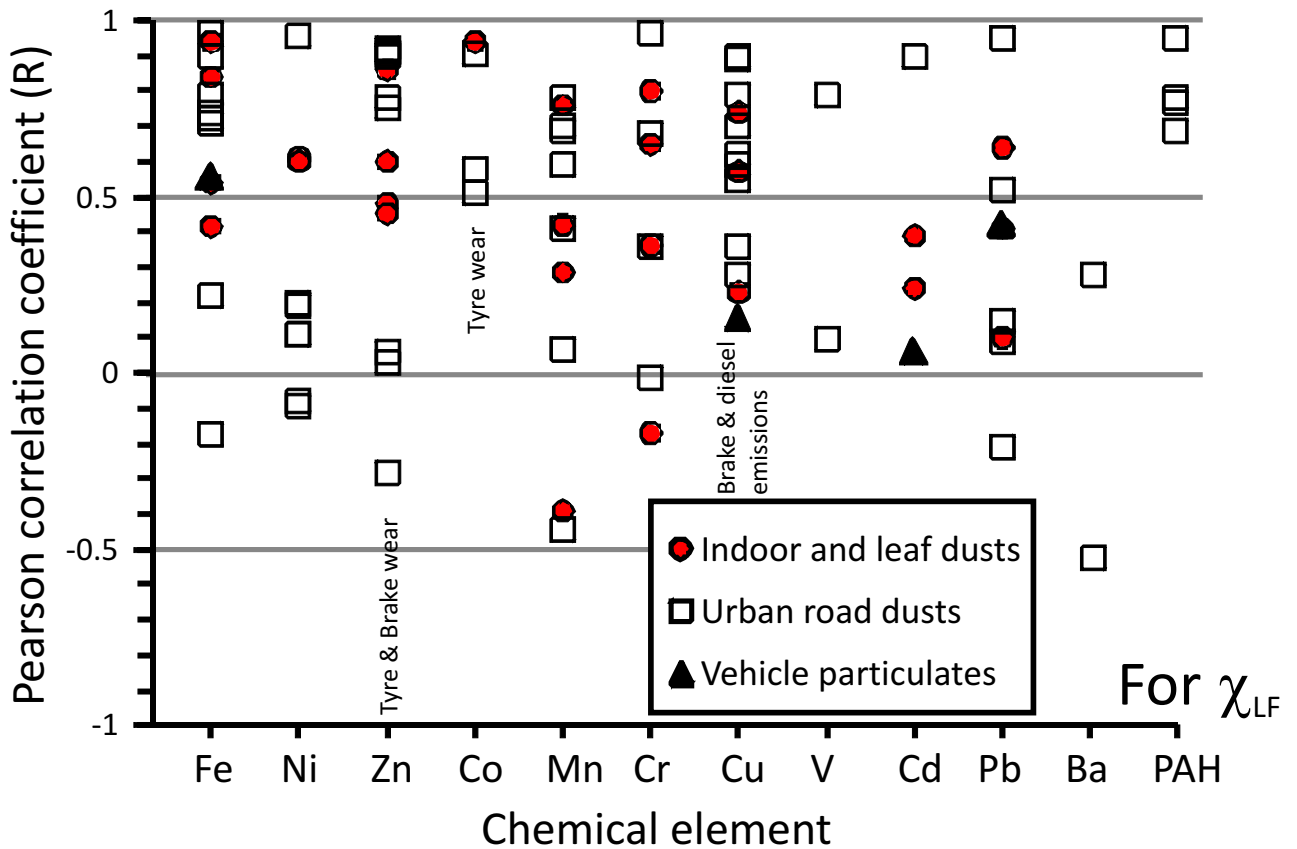
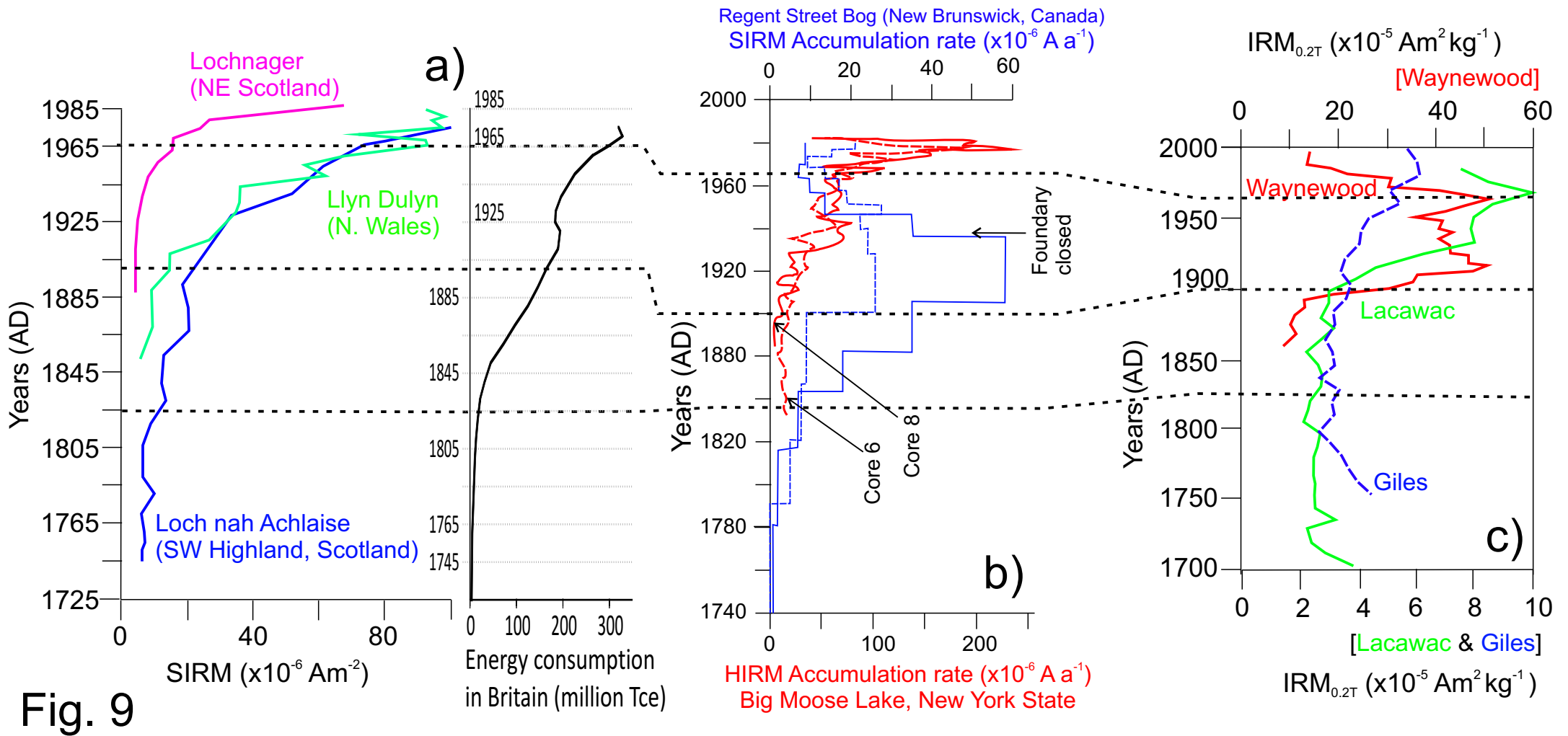


Fig. 8





**Fig. 9**